Limit Analysis of Stability of Circular Foundation Pit

CUI XINZHUANG, YAO ZHANYONG, JIN QING, WU SHIMEI
School of Civil Engineering
Shandong University
School of Civil Engineering, South Campus of Shandong University, Jingshi Road 73#, Jinan, 250061
China

Abstract: Circular foundation pits often appear in civil engineering. In order to obtain the critical depth of the non-supported circular foundation pit, the upper-bound method in plasticity mechanics was employed. The assumed slip surface in analysis was the rotational logspiral surface. The kinematically admissible velocity field was obtained according to the associated flow rule for Coulomb material, and the optimization model of the critical depth was established and solved with SQP optimization algorithm. The variations of the critical depth with the slope angle, the ratio of depth to radius of pit and the internal friction angle of soil were studied. The arch effect of the circular foundation pit makes the critical depth larger than the critical height of the plane slope; however, when the ratio of depth to radius of pit approaches zero, the upper-bound solution of the former approaches that of the latter. If the ratio of depth to diameter of pit is less than 10, the arch effect may be ignored and the foundation pit can be analyzed as the plane slope with the method of slices. Comparison between upper-bound solution and the solution from limit equilibrium method showed that the former is closer to the true solution than the latter.

Key-Words: circular foundation pit; slope; critical depth; limit analysis; upper-bound method; arch effect

1 Introduction

Limit analysis theory is an important branch of plastic mechanics. It was developed from the metal plastic theory and has already been extended to rock and soil mechanics now. Limit analysis was used to solve some engineering problems, such as slope stability and limit load[1-4]. It contains two kinds of basic methods, i.e. the upper-bound method and the lower-bound method. Based on upper-bound theorem, the upper-bound method needs to establish the kinematically admissible failure mechanism and velocity field in advance. The velocity field must meet motion boundary conditions and associated plastic flow rule. Based on lower-bound theorem, the lower-bound method needs to set up statically admissible stress field which must satisfy equilibrium equation, stress boundary condition and not disobey the failure criterion which is Mohr-Coulomb failure criterion for rock and soil.

Limit analysis can give the definite bounds of some problems such as the slope critical height and the pile bearing capacity[1-3]. However, the solution from rigid limit equilibrium method, which is another analysis method used extensively in geomechanics, is difficult to tell that it is a upper-bound solution or lower-bound solution.

For Some failure mechanisms used in limit equilibrium method, the corresponding kinematically admissible velocity fields for limit analysis can be obtained according to virtual work principle. So the limit equilibrium solutions from these failure mechanisms are upper-bound solutions, just as the Sarma method which is an important method solving the safety factor of slope. But for Some failure mechanisms used frequently in limit equilibrium method, the corresponding kinematically admissible velocity field can’t be set up, so the limit equilibrium solutions aren’t upper-bound solutions, just as the vertical slices method and the circular slide method used for the stability analysis of slope. For vertical slices method, inter-slice force can’t satisfy Mohr-Coulomb failure criterion. For Coulomb material obeying associated flow rule, the angle between velocity jump vector and the tangent of the slip surface should be equal to the internal friction angle of material, but for the circular rigid slide mechanism, we can’t set up any velocity field satisfying this.

In addition, the limit equilibrium solutions can’t be used as the lower-bound solution because the stress field in rigid body is not known.

The upper-bound method is applied more extensively than the lower-bound method because the establishment of statically admissible stress field is rather difficult. While solving the problem with the upper-bound method, a valid failure mechanism is assumed firstly, and then the internal energy dissipation rate and the work done by external loads are calculated respectively and equated with each other. Thus a serial of upper-bound solutions corresponding to the specific mechanism are obtained, and finally, the optimum upper-bound solution can be gotten by employing optimization technology[5]. Donald I and Chen Z Y studied the stabilities of plan strain and three-dimension slopes using rigid blocks translational failure mechanism[1-2]. Murff obtained the lateral bearing capacity of pile with three-dimensional deforming mechanism[3]. However, limit analysis hasn't be used to solve the axisymetrical problem as yet. Axisymetrical problems appear frequently in geotchnical engineering such as the stabilities of circular foundation pit and most in-situ tests such as CPT and SPT. The aim of this paper is to solve the non-supported critical depth of the circular foundation pit to demonstrate the application of upper-bound method to axisymetrical problem. The circular foundation pit is often analyzed as the plane strain problem when the ratio of depth to radius of pit is large enough. When the ratio of depth to radius of pit is small, however, the plane strain solution is not accurate because the arch effect of soil mass largely enhances the stability of the pit.

Using axisymetrical split line theory, Верезанцев В Г obtained the approximate active earth pressure on retaining wall of circular foundation pit [6]. Through integrating the earth pressure along the depth and equating the integral zero, Ma S C [7] obtained the limit equilibrium solution of critical depth of circular foundation pit. In this paper, limit analysis method will be employed to solve the critical depth of the circular foundation pit. In analysis, soil is assumed homogeneous and isotropic, and the failure is axisymetrical.

2 Problem Formulation

2.1 Failure Mechanism

As a kind of slope, the common failure surface of circular foundation pit is logspiral surface, just as shown in figure 1. The rotating center of failure face is on the axis of foundation pit. The function of logspiral surface is:

$$r = r_0 e^{(\theta-\theta_0)\tan\phi} \tag{1}$$

Where ϕ is internal friction angle of soil; r_0 is polar radius of point b where $\theta = \theta_0$.

The shape of foundation pit can be described with the ratio of depth to bottom radius D/R and slope angle α of foundation pit, as shown in figure 1. Once they are known, the dimension of the whole failure zone can be determined by two independent variables: the characteristic angle θ_0 and the depth of foundation pit D.

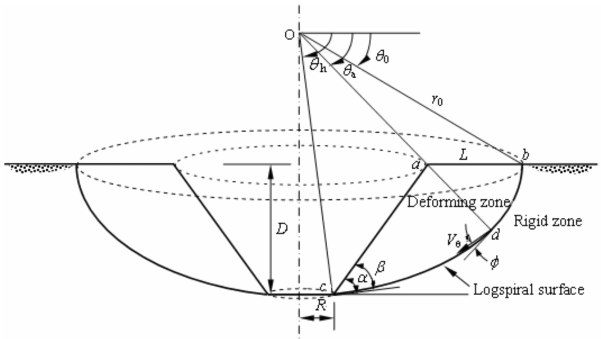

Fig.1 Failure mechanism of circular foundation pit

In Fig.1, L is the length of ab; β is defined as split angle that is the angle between slip surface and pit wall at slope toe. Let $A = D/r_0$ and $B = L/r_0$. Then equations (2)-(4) can be derived from Fig.1:

$$A = \sin\theta_h \cdot e^{(\theta_h-\theta_0)\tan\phi} - \sin\theta_0 \tag{2}$$

$$B = \cos\theta_0 - \cos\theta_h \cdot e^{(\theta_h-\theta_0)\tan\phi} - A\cdot\cot\alpha \tag{3}$$

$$\beta = \theta_h - \phi + \alpha - \pi/2 \tag{4}$$

The function of the line ab is:

$$r = \frac{\sin\theta_0}{\sin\theta} r_0 \tag{5}$$

The function of the line ac is:

$$r = \frac{\sin\theta_0 + \tan\alpha\cdot(\cos\theta_0 - B)}{\sin\theta + \tan\alpha\cdot\cos\theta} r_0 \tag{6}$$

The polar angle of the point a is:

$$\theta_a = arc\cot\frac{\cos\theta_0 - B}{\sin\theta_0} \tag{7}$$

According to geometrical relationship, θ_h can be obtained from the following equation:

$$\frac{D}{R} = \frac{\sin\theta_h e^{(\theta_h-\theta_0)\tan\phi}\cos\theta_h}{\sin\theta_h e^{(\theta_h-\theta_0)\tan\phi} - \sin\theta_0} \tag{8}$$

2.2 Velocity Field

V_r , V_θ and V_ψ are radial, tangential and circumferential velocity components in spherical coordinate system (r,θ,ψ) , respectively. According to the associated plastic flow rule, $V_r = V_\psi = 0$ on the logspiral failure surface. Here we assume further that $V_r = V_\psi = 0$ in the whole deforming region. V_θ can be determined according to the associated plastic flow rule. In spherical coordinates, tensor- strain-rates are written as:

$$\left.\begin{aligned} \dot{\varepsilon}_r &= 0 \\ \dot{\varepsilon}_\theta &= \frac{1}{r}\frac{\partial V_\theta}{\partial \theta} \\ \dot{\varepsilon}_\psi &= \frac{\cot\theta}{r} V_\theta \\ \dot{\gamma}_{r\theta} &= \frac{1}{2}\left(\frac{\partial V_\theta}{\partial r} - \frac{V_\theta}{r}\right) \\ \dot{\gamma}_{r\psi} &= 0 \\ \dot{\gamma}_{\theta\psi} &= 0 \end{aligned}\right\} \tag{9}$$

Because $\dot{\gamma}_{r\psi} = \dot{\gamma}_{\theta\psi} = 0$, $\dot{\varepsilon}_\psi$ is principal strain rate. According to the normality of $\dot{\varepsilon}_r$, $\dot{\varepsilon}_\theta$ and $\dot{\varepsilon}_\psi$, we know $\dot{\varepsilon}_r$ and $\dot{\varepsilon}_\theta$ are also principal strain rates. Subsequently we can know:

$$\dot{\gamma}_{r\theta} = \frac{1}{2}\left(\frac{\partial V_\theta}{\partial r} - \frac{V_\theta}{r}\right) = 0$$

(10)

For Coulomb material matching associated flow rule, Chen W F gave the following equation[5]:

$$T \cdot \sum \dot{\varepsilon}_t + \sum \dot{\varepsilon}_c = 0$$

(11)

Where $T = \tan^2(\frac{\pi}{4} - \frac{\phi}{2})$, $\sum \dot{\varepsilon}_t$ and $\sum \dot{\varepsilon}_c$ are the summation of principal tensional strain rates and the summation of principal compressive strain rates, respectively. Note that compressive strain rates are positive in this paper.

Because $\dot{\varepsilon}_r = 0$, we know from equation (11) that there is a maximum strain rate $\dot{\varepsilon}_{\max}$ and a minimum strain rate $\dot{\varepsilon}_{\min}$ in $\dot{\varepsilon}_\theta$ and $\dot{\varepsilon}_\psi$. In order to obtain velocity field, we studied the following two cases.

(1) $\dot{\varepsilon}_\psi = \dot{\varepsilon}_{\max}$, $\dot{\varepsilon}_\theta = \dot{\varepsilon}_{\min}$

From Eq.(9) and Eq.(10), we obtain:

$$T \cot\theta V_\theta + \frac{\partial V_\theta}{\partial \theta} = 0 \tag{12}$$

From Eq.(10) and Eq.(12), we obtain:

$$T \cdot r \cot\theta \frac{\partial V_\theta}{\partial r} + \frac{\partial V_\theta}{\partial \theta} = 0 \tag{13}$$

The partial differential equations above can be solved using the variable separation method. Let $V_\theta = f(\theta) \cdot g(r)$, and substitute it into Eq.(13) and obtain:

$$\frac{rf'(r)}{f(r)} = -\frac{g'(\theta)}{g(\theta)}\frac{\tan\theta}{T} = C_1 \tag{14}$$

Where C_1 is a constant.

Solving the two ordinary differential equations in Eq.(14), $f(r)$ and $g(\theta)$ can be obtained. The final expression of V_θ is:

$$V_\theta = f(r)g(\theta) = Cr^{C_1} \sin^{-TC_1}\theta \tag{15}$$

Where C is a constant.

Substituting Eq.(15) into Eq.(10) or Eq.(12) leads to $C_1 = 1$, thus Eq.(15) can be written as

$$V_\theta = Cr \sin^{-T}\theta \tag{16}$$

Because $\dot{\varepsilon}_\psi = \dot{\varepsilon}_{\max} > 0$, we can know $C > 0$ after substituting Eq.(16) into Eq.(9). At the same time, $0 < \theta < \frac{\pi}{2}$. So we can know $V_\theta > 0$. This indicates that soil mass slides down and doesn't disobey the true physical case.

(2) $\dot{\varepsilon}_\theta = \dot{\varepsilon}_{\max}$, $\dot{\varepsilon}_\psi = \dot{\varepsilon}_{\min}$

Using the same methods, we obtain:

$$V_\theta = Cr \sin^{-\frac{1}{T}}\theta \tag{17}$$

Because $\dot{\varepsilon}_\psi = \dot{\varepsilon}_{\min} < 0$, $C < 0$ can be known after substituting Eq.(17) into Eq.(9). At the same time, $0 < \theta < \frac{\pi}{2}$. so we can obtain $V_\theta < 0$. This implies that soil mass slides up and disobeys the true physical condition.

Now we know that the maximum and minimum principal strain rate are $\dot{\varepsilon}_\psi$ and $\dot{\varepsilon}_\theta$, respectively, and V_θ is determined uniquely by Eq. (16).

2.3 Internal Energy Dissipation Rate and Work by External Force

The internal energy dissipation rates include those on failure surface and in plasticity deforming zone. According to the literature [5], the energy dissipation rate of unit area on failure surface is calculated with the following equation:

$$\dot{E} = cV_s \tag{18}$$

Where c is cohesion of soil; V_s is tangential velocity jump across the failure surface.

Literature [5] also gave the expression of the internal energy dissipation rate of unit volume in plasticity deforming zone:

$$\dot{E} = 2c\sqrt{T}\sum \dot{\varepsilon}_t \quad (19)$$

Once velocity field is known, strain rate field can be obtained according to geometric equations. But it's difficult to obtain the analytic expression of principal strain rates and this limits the application of Eq.(19). Cui et al derived the general solution of the energy dissipation rate of unit volume in plasticity deforming region in terms of bulk strain rate [8]:

$$\dot{E} = c\cot\phi\dot{\varepsilon}_V \quad (20)$$

The energy dissipation rate of unit volume in deforming region can be obtained from Eq.(9) and Eq.(20):

$$\dot{E} = Cc(1-T)\cot\phi\cot\theta\sin^{-T}\theta \quad (21)$$

For the foundation pit studied in this paper, the gravity of soil is the only external force. The gravity work rate of unit volume soil is expressed:

$$\dot{w} = \gamma V_\theta \cos\theta \quad (22)$$

Where γ is soil bulk density.

The total energy dissipation rate on failure surface $\dot{D}_1$ is obtained by integrating Eq.(18) along the surface that is gotten by rotating the logspiral line bc about the axes of foundation pit, as shown in Fig.1. The total internal energy dissipation rate in deforming region $\dot{D}_2$ and the gravity work rate of soil mass $\dot{W}$ can be obtained by integrating Eq.(21) and Eq.(22), respectively, in the annular domain that is obtained by rotating the area abc about the axes of foundation pit, as shown in Fig.1. The integrations above have no analytic solution, so we need to employ numerical methods to solve them.

2.4 Mathematic Model

According to upper-bound theorem, there is

$$\dot{D}_1 + \dot{D}_2 = \dot{W} \quad (23)$$

The critical depth of foundation pit can be expressed as:

$$D_{cr} = \frac{c}{\gamma} f(\theta_0) \quad (24)$$

In order to obtain the minimum upper-bound solution of critical depth, we need to solve the minimum of function $f(\theta_0)$. Let $N_s = \min f(\theta_0)$, where N_s is a dimensionless variable, independent of c and γ and only related to ϕ, α and D/R. The mathematic model used to solve the minimum upper-bound solution of critical depth of foundation pit is as follows:

$$\left.\begin{array}{r} N_s = \min f(\theta_0) \\ B \geq 0 \end{array}\right\} \quad (25)$$

The constraint condition in Eq.(25) makes sure that point b is on the right of point a as shown in Fig.1. Base on SQP optimization algorithm, we used matlab software to solve the minimum upper-bound of critical depth of circular foundation pit.

3 Results and Analysises

When D/R is equal to 0.1 and 1.0, respectively, the variations of N_s with ϕ and α are showed in Fig.2. N_s increases with the increment of ϕ. Moreover, the bigger ϕ is, the more rapidly N_s varies. N_s decreases with the increment of α , furthermore, the smaller α is, the more rapidly N_s varies.

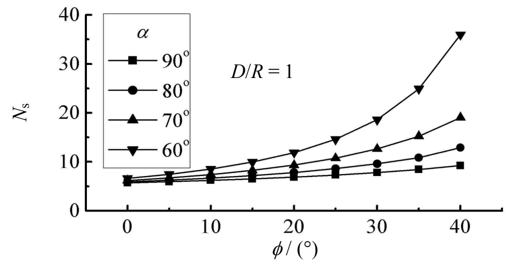

(a) $D/R = 1$

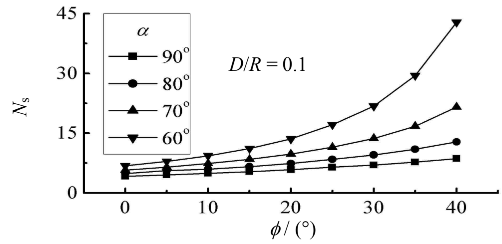

(b) $D/R = 0.1$

Fig.2 Variations of N_s with ϕ and α

Fig.3 shows variations of N_s with D/R and ϕ when $\alpha = 90^\circ$. N_s increases with the increment of D/R. Moreover, when D/R is very small, the variation of N_s is also small. This shows that the arch effect of soil mass largely enhances the stability of the foundation pit.

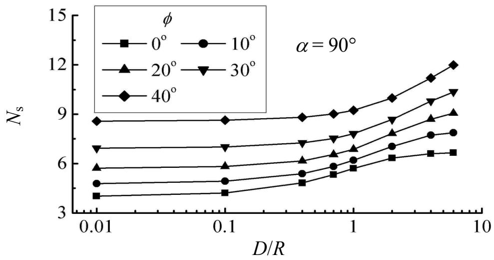

Fig.3 Variations of N_s with D/R and ϕ

Fig.4 shows variations of characteristic angle θ_0 with ϕ and α . θ_0 increases with the increments of ϕ and α . Once θ_0 and N_s are known, other characteristic angles θ_a and θ_h and characteristic dimensions such as r_0 , L and so on can all be obtained. Thus the location and shape of the slip surface can be decided.

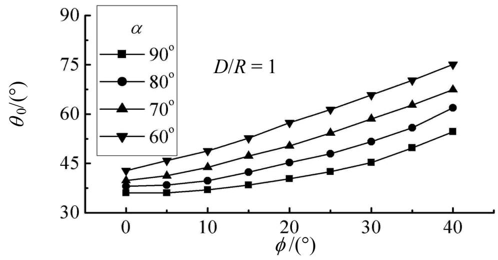

Fig.4 Variations of θ_0 with ϕ and α

When D/R is very small, the circular foundation pit can be analyzed as the plane slope. In limit analysis of plane slope, two kinds of failure mechanisms are usually used, i.e. rigid blocks translational and rotational mechanisms, as shown in fig. 5 and fig. 6, respectively. In table 1, N_s of vertical circular foundation pit with $D/R = 0.001$ and vertical plane slope from different failure mechanisms are given, respectively. When D/R is very small, it can be found that N_s of circular foundation pit approximates that of plan slope from rigid blocks translational mechanism, and both of them are slightly greater than that from rigid blocks rotational mechanism.

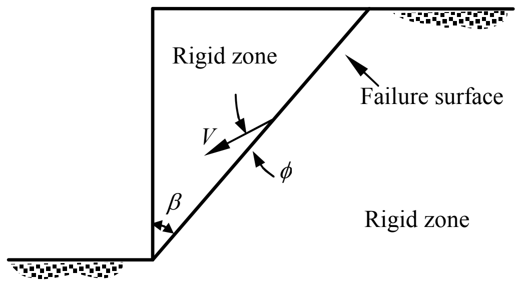

Fig.5 Rigid blocks translational failure mechanism

According to the results computed with the method proposed in this paper, we also know that $\theta_0 \to \theta_h$ when $D/R \to 0$. This implies that the rotational logspiral surface degenerates to the circular truncated surface. At the same time, the critical slip angle β_{cr} corresponding to D_{cr} is the same as the critical value of β shown in Fig.5 and both are equal to $(\pi/4 - \phi/2)$. But this doesn't imply that the plasticity deforming region degenerates to rigid region because internal energy dissipation rate expressed by Eq. (9) isn't equal to zero.

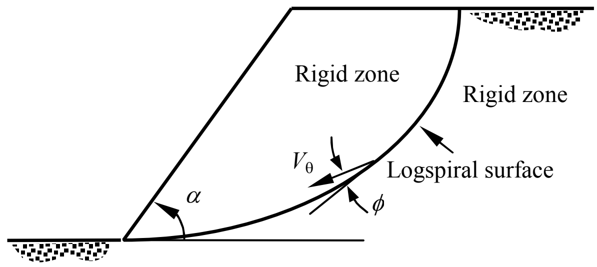

Fig.6 Rigid blocks rotational failure mechanism

Table 1 N_s obtained from some failure mechanisms

ϕ	N_s: Plane slope with rigid blocks translational failure mechanism	Plane slope with rigid blocks rotational failure mechanism	Circular foundation pit of D/R=0.001 with axisymetrical failure mechanism
0°	4.000	3.8300	4.0021
10°	4.7666	4.5925	4.7685
20°	5.7115	5.5116	5.7229
30°	6.9261	6.6935	6.9289
40°	8.5741	8.3330	8.5785

The stability of plane slope often be analyzed with vertical slices method, e.g. Janbu method. For plan slope, when $\phi = 20^\circ$, N_s from Janbu method is equal to 6.01. It is very similar to the upper limit solution of circular foundation pit whose D/R is 0.2. So the arch effect of the foundation pit may be ignored and it can be regarded as plan slope and analyzed with the slices method when the ratio of depth to diameter of pit is less than 10.

Comparison was made between upper-bound solution and limit equilibrium solution obtained by Ma S C [7], as shown in Fig 7. It can be seen that upper-bound solution is slightly greater than limit equilibrium solution when $\phi = 0$, however, in other cases, the former is always less than the latter. This implies that the upper-bound solution is better than limit equilibrium solution and closer to the true solution than the latter generally.

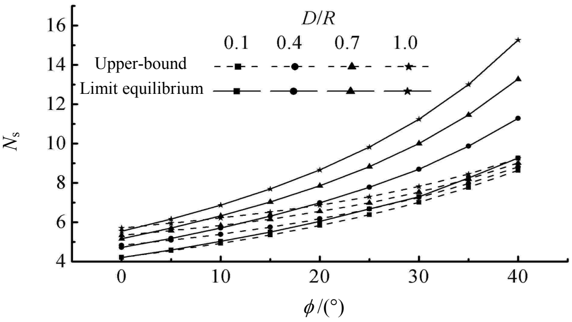

Fig.7 Comparison between upper-bound and limit equilibrium solution of critical depth

4 Conclusion

Assuming that soil mass is homogeneous and isotropic and the failure model of circular foundation pit is axisymetrical, kinematically admissible failure mechanism and velocity field were established according to associated plastic flow rule. Using them, the stability of the circular foundation pit was analyzed and the limit upper-bound solution of critical height was obtained. The following are some important conclusions:

(1) Critical depth increases with the decrement of slope angle of foundation pit and the increment of the ratio of depth to radius and internal friction angle of soil.

(2) The arch effect of circular foundation pit makes its critical depth greater than the critical height of plane slope. However, the arch effect is unconspicuous when the ratio of depth to diameter of pit is less than 10.

(3) When the ratio of depth to radius is very small, the upper-bound solution of circular foundation pit is very close to the one of plane slope obtained from rigid blocks translational failure mechanism. Moreover, on the axisymetrical surface, the rotational logspiral failure line degenerates to straight line, and the critical slip angle is the same as plane slope from rigid blocks translational mechanism, however, the plasticity deforming zone isn't rigid yet.

(4) By comparison between upper-bound solution and limit equilibrium solution, it was found that the former is closer to the true solution than the latter.

5 Acknowledgements

This work was supported by Natural Science Foundation of Shandong Province, China(No. Q2006F02).

References:

[1] Donald I, Chen Z Y. Slope stability analysis by the upper-bound approach: fundamentals and methods. *Canadian Geotechnical Journal*, Vol.34, No.6, 1997, pp. 853-862

[2] Chen Z Y, Wang X G, Haberfield C, et al. A three-dimensional slope stability analysis method using the upper-bound theorem –Part □: theory and methods. *International Journal of Rock Mechanics and Mining Sciences*, Vol.38, No.6, 2001, pp. 369-378

[3] Murff J D, Hamilton J M. P-ultimate for undrained analysis of laterally loaded piles. *Journal of Geotechnical Engineering*, Vol.119, No.1, 1993 , pp.91-107

[4] Drescher A, Detourany E. Limit load in translational failure mechanism for associative non-associative materials. *Geotechnique*, Vol.43, No.3, 1993, pp.443-456

[5] Chen W F. *Limit analysis and soil plasticity*. Amsterdam, the Netherlands: Elsevier Publishing Co., 1975

[6] Березанцев В Г. *Axial-symmetrical limit equilibrium problems of loose media*. Beijing: China Architecture and Building Press, 1981

[7] Ma S C, Zou Y S, Wang Y S. Critical height calculation of upright non-supported circular foundation pit. *Natural Science Journal of Xiangtan University*, Vol.24, No.2 , 2002, pp. 88-90

[8] Cui X Z, Jin Q, Shang Q S, et al. General solving method of energy dissipation rate of deforming region in upper-bound analysis for Coulomb material. *Key Engineering Materials*, Vols 306-308, 2006, pp.1439-1444